

Microstructure dependence of microwave dielectric characteristics in $\text{Ba}_{6-3x}\text{Sm}_{8+2x}\text{Ti}_{18}\text{O}_{54}$ ($x=2/3$) ceramics

N. Qin · X. M. Chen

Published online: 29 March 2007
© Springer Science + Business Media, LLC 2007

Abstract Effects of microstructures on the microwave dielectric characteristics of $\text{Ba}_{6-3x}\text{Sm}_{8+2x}\text{Ti}_{18}\text{O}_{54}$ ($x=2/3$) ceramics were investigated by controlling the sintering process and the annealing condition. The dielectric constant was sensitive to the porosity in ceramics, but insensitive to the annealing process. Qf value varied with both the annealing atmosphere and the sintering temperature, which indicates the strong reliance of dielectric loss on defects and grain boundaries. τ_f value exhibited a complex dependence on the sintering temperature. The orientation of grains is responsible for the variation of τ_f .

Keywords Microwave dielectric properties · Microstructure · Tungsten bronze type · Annealing atmosphere

1 Introduction

The new tungsten bronze-type $\text{Ba}_{6-3x}\text{Ln}_{8+2x}\text{Ti}_{18}\text{O}_{54}$ (Ln = La, Nd and Sm) ceramics have the typical microwave dielectric properties ($\epsilon=78\sim 110$, $Qf=2,000\sim 10,500$ GHz, $\tau_f=-15\sim +400$ ppm/ $^{\circ}\text{C}$) for microwave resonators and filters [1]. In the light of current understanding, three intrinsic factors are essential to the microwave dielectric properties of perovskite-like ceramics: the polarizability of the cations, the tilting angle, and the volume of TiO_6 octahedra [2–5]. Most of the work has been focused on

improving the microwave dielectric properties by ionic substitution. The effect of microstructures, which dominates the extrinsic dielectric properties, has been less regarded.

Recently, some efforts were conducted to modify the microwave dielectric properties of $\text{Ba}_{6-3x}\text{Ln}_{8+2x}\text{Ti}_{18}\text{O}_{54}$ ceramics by controlling the microstructure. Li *et al.* [6] reported the sintering time dependence of microstructure and microwave dielectric properties of $\text{Ba}_{6-3x}(\text{Sm}_{1-y}\text{Nd}_y)_{8+2x}\text{Ti}_{18}\text{O}_{54}$ ceramics. Negas *et al.* [7] discussed the influence of grain orientation on the microwave dielectric properties of $\text{Ba}_{6-3x}\text{Ln}_{8+2x}\text{Ti}_{18}\text{O}_{54}$ ceramics. Wada *et al.* [8] and Hoffman *et al.* [9] fabricated the anisotropic $\text{Ba}_{6-3x}\text{Sm}_{8+2x}\text{Ti}_{18}\text{O}_{54}$ ceramics by controlling the grain orientation through template grain growth technique and hot-press sintering, respectively. The microwave dielectric properties were found sensitive to grain orientation degree and the measuring direction. However, the relationship between microstructure and microwave dielectric properties is still ambiguous.

To clarify this problem, the microstructures of $\text{Ba}_{6-3x}\text{Sm}_{8+2x}\text{Ti}_{18}\text{O}_{54}$ ($x=2/3$) ceramics were modified by controlling the sintering and the annealing situation. The microwave dielectric properties were discussed in relation to the microstructure features including porosity, defects, and grain morphology.

2 Experimental procedure

$\text{Ba}_{6-3x}\text{Sm}_{8+2x}\text{Ti}_{18}\text{O}_{54}$ ($x=2/3$) powders were prepared by a solid-state reaction method using BaCO_3 (99.95%), Sm_2O_3 (99.5%), and TiO_2 (99.5%) as the raw materials. The powders were weighed and ball-milled with zirconia in ethanol for 24 h. The dried mixture was calcined at 1,200 $^{\circ}\text{C}$ in air for 3 h. After being ball-milled again, the powders

N. Qin · X. M. Chen (✉)
Department of Materials Science and Engineering,
Zhejiang University,
38 Zheda Road,
Hangzhou 310027, China
e-mail: xmchen@cmsce.zju.edu.cn

were gridded with 10 wt% of PVA and were pressed uniaxially into $\phi 12 \times 6$ mm cylinders. The compacts were sintered at 1,250–1,500°C in air for 3 h. Then, they were cooled down slowly at a rate of 2°C/min. The annealing processes were performed at 1,150°C for 5 h in O₂ atmosphere and at 1,000°C for 5 h in N₂ atmosphere, respectively.

Dilatometry data for the sintering of Ba_{6–3x}Sm_{8+2x}Ti₁₈O₅₄ green compact in the size of $\phi 12 \times 5$ mm was obtained by a dilatometer (Linseis, German) with a constant heating rate of 10°C/min. The apparent density was measured by Archimedes' method, and the relative density was calculated by comparing the measured data with the theoretical one. Phase constitution of the sintered samples was identified by x-ray diffraction (XRD) pattern. Microstructures of the ceramics were observed by scanning electron microscopy (SEM). The samples for SEM observation were polished and thermally etched at 1,280°C for 1 h. The microwave dielectric properties were evaluated at 3–4 GHz by an S-parameter network analyzer (Agilent 8753ES) using Hakki and Coleman's resonator method [10]. The temperature coefficient of resonant frequency (τ_f) was measured in a temperature range from –50 to 85°C.

3 Results and discussion

Figure 1 plots the dilatometry data for the sintering of Ba_{6–3x}Sm_{8+2x}Ti₁₈O₅₄ ($x=2/3$) ceramics. Shrinkage occurs at about 1,200°C and the shrinkage rate, defined as the first-order differential coefficient of shrinkage on time $d(\Delta L)/(L_0 dt)$, peaks approximately at 1,300°C. According to the densification curve in Fig. 2, the ceramics were well sintered in a wide temperature range from 1,300 to 1,450°C and became over-sintered when heated to 1,500°C.

No secondary phase was detected by XRD analysis over the whole sintering temperature range. As can be seen in the

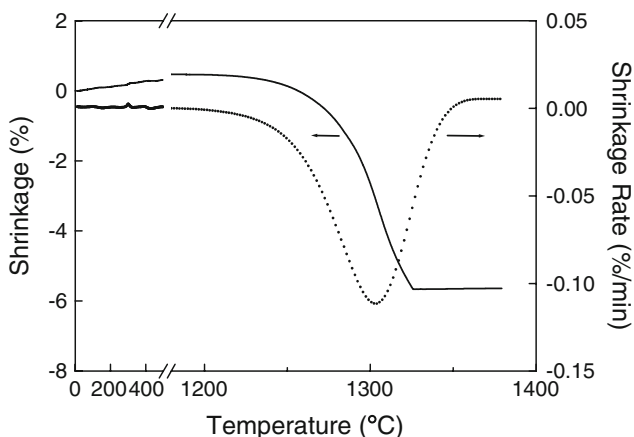


Fig. 1 Dilatometer measured shrinkage versus temperature for Ba_{6–3x}Sm_{8+2x}Ti₁₈O₅₄ ($x=2/3$) sintered at a constant heating rate of 10°C/min

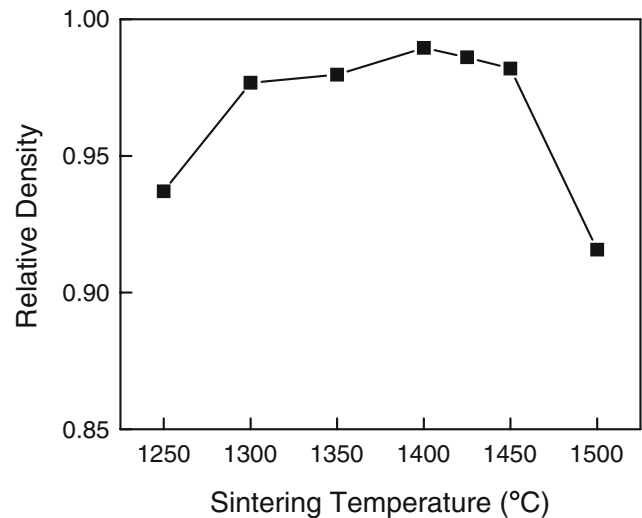


Fig. 2 Density of Ba_{6–3x}Sm_{8+2x}Ti₁₈O₅₄ ($x=2/3$) ceramics as a function of sintering temperature

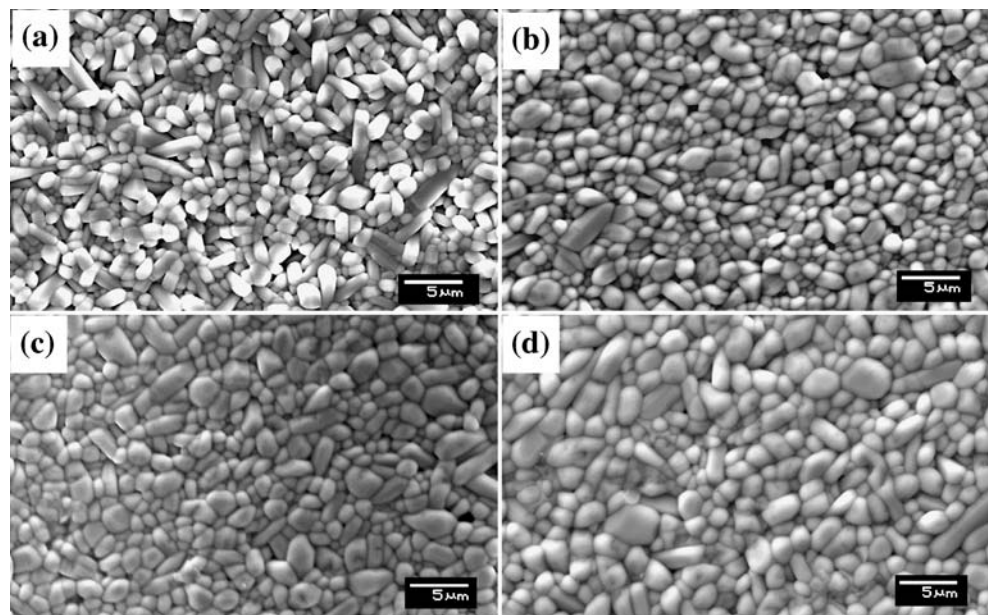
SEM graphs (Fig. 3), the rod-like grains elongate along the shortest *c*-axis with increasing sintering temperature, accompanied with the increase in grain size. The morphologic features of the grains were characterized using a public domain program NIH Image J¹. A multistep digital image processing [11] was performed to extract and close the grain boundaries from the digital SEM images. The outlined grains were measured in pixels. Some statistical results (grain area, perimeter, mean diameter, circularity) are summarized and compared in Table 1, where the mean diameter (*d*) of an individual grain is calculated from the outlined area (*A*) by equation $d = 2\sqrt{A/\pi}$ and the average value is adopted. The grain shape is characterized by the parameter “circularity” (defined as $4\pi(\text{area}/\text{perimeter}^2)$). A value of 1 indicates a perfect circle. As shown in Fig. 4, the average circularity of the grains decreases from 1 with sintering temperature, in accordance with the elongated grain growth.

Because Ti⁴⁺ were partially reduced to Ti³⁺, the inner part of the ceramics changed from yellow to black after being annealed in nitrogen. Some oxygen vacancies were created to equilibrate the local valance. The concentration of oxygen vacancies was evaluated by measuring the weight loss of the annealed samples. Nearly 0.4 mol% oxygen atoms were lost in N₂-annealed ceramics. While, the oxygen concentration was not changed in O₂-annealed samples.

Microwave dielectric properties of the present ceramics are summarized in Table 2 and plotted in Fig. 5. The dielectric constant increases with increasing sintering temperature and achieves the maximum value at 1,400°C. Meanwhile, the *Qf* value increases initially and exhibits a platform in the sintering temperature range of 1,350–1,450°C.

¹ NIH Image J public domain program is conducted by Wayne Rasband from the National Institutes of Health (<http://rsb.info.nih.gov/ij>)

Fig. 3 SEM micrographs on the polished and thermally etched surface of $\text{Ba}_{6-3x}\text{Sm}_{8+2x}\text{Ti}_{18}\text{O}_{54}$ ($x=2/3$) ceramics, which were sintered at (a) 1,300°C, (b) 1,350°C, (c) 1,400°C and (d) 1,450°C for 3 h, respectively



Due to the over-sintering at 1,500°C, the Qf value decreased sharply. The variation of τ_f is much more complex compared with the other two characteristics. It decreases at first and then shifts towards zero with the increasing sintering temperature. Both the annealing processes in O_2 and N_2 show no evident effect on dielectric constant. The Qf value was obviously reduced by N_2 -annealing and was not influenced by O_2 -annealing. The relationship between microstructure and microwave dielectric properties will be discussed in the following paragraphs.

The dielectric constant is defined as the macro polarizability of materials. At microwave frequencies, the ionic displacement and the distortion of electron cloud dominate the electric polarization. The slow polarization mechanisms such as ionic-jumping, conduction losses, and interfacial polarization are unable to respond. Consequently, the effect of grain boundaries, micro-cracks, and defects can be neglected at microwave frequency. It is evident from early studies that the dielectric constant is sensitive to the phase constitution. The pores in the host materials can be seen as a secondary phase. Because the relative dielectric constant

Table 1 Descriptive statistics data to grain size and morphology measurements.

T_s (°C)	Parameters			
	Area (μm^2)	Perimeter (μm)	Diameter (μm)	Circularity
1,300	0.655	0.675	0.806	0.675
1,350	0.779	0.650	0.887	0.650
1,400	1.656	5.319	1.289	0.619
1,450	1.748	5.659	1.284	0.571

T_s : sintering temperature

of ceramics is usually much higher than that of the air (~ 1), the increase in porosity will lead to the obvious decrease in the composite dielectric constant. Various dielectric mixing laws were proposed to express the dielectric constant of the air-ceramic composite. In the effective medium approximation, the dielectric constant is given as [12]

$$R \frac{\epsilon_{\text{cer}} - \epsilon_{\text{m}}}{\epsilon_{\text{cer}} + 2\epsilon_{\text{m}}} + (1 - R) \frac{\epsilon_0 - \epsilon_{\text{m}}}{\epsilon_0 + 2\epsilon_{\text{m}}} = 0, \quad (1)$$

where, R is the relative density of the ceramic, ϵ_0 and ϵ_{cer} are defined as the dielectric constant of air and the ceramic. As shown in Fig. 6, the calculated dielectric constant is well

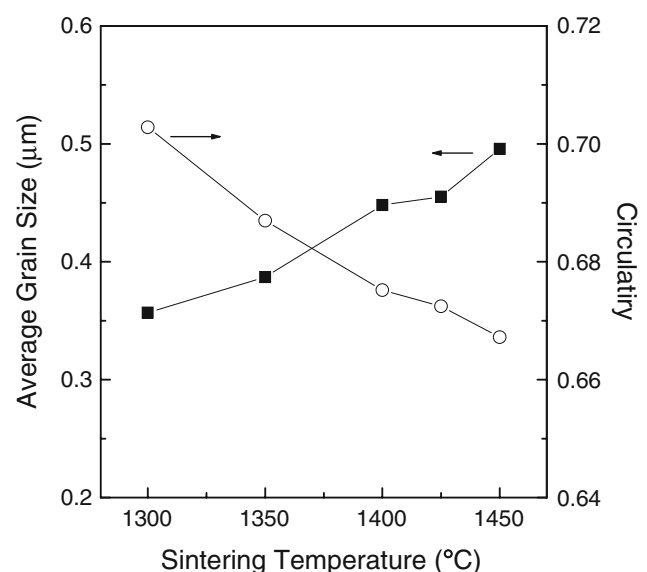


Fig. 4 The average grain size and circularity as functions of sintering temperature for $\text{Ba}_{6-3x}\text{Sm}_{8+2x}\text{Ti}_{18}\text{O}_{54}$ ($x=2/3$) ceramics

Table 2 Microwave dielectric properties of $Ba_{6-3x}Sm_{8+2x}Ti_{18}O_{54}$ ($x=2/3$) ceramics.

T_s (°C)	Annealing condition	Microwave dielectric properties		
		ϵ_r	Qf (GHz)	τ_f (ppm/°C)
1,300	As sintered	77.4	8,852	-2.2
1,350	As sintered	79.9	10,166	-12.8
1,400	As sintered	81.7	10,229	-7.7
1,425	As sintered	80.7	10,209	-1.4
1,450	As sintered	80.5	10,076	-4.2
1,500	As sintered	67.2	4,545	
1,300	O ₂ , 1,150°C	77.3	8,650	-10.7
1,350	O ₂ , 1,150°C	80.2	10,132	-17.4
1,400	O ₂ , 1,150°C	81.0	10,125	-7.1
1,425	O ₂ , 1,150°C	81.7	10,066	-3.5
1,450	O ₂ , 1,150°C	80.3	10,073	-2.2
1,300	N ₂ , 1,000°C	77.3	3,061	-14.7
1,450	N ₂ , 1,000°C	80.3	1,691	+12.0

fitted with the experimental data. It has been mentioned that the annealing process has no effect on the dielectric constant, which indicates that the dielectric constant is insensitive to the micro-defects.

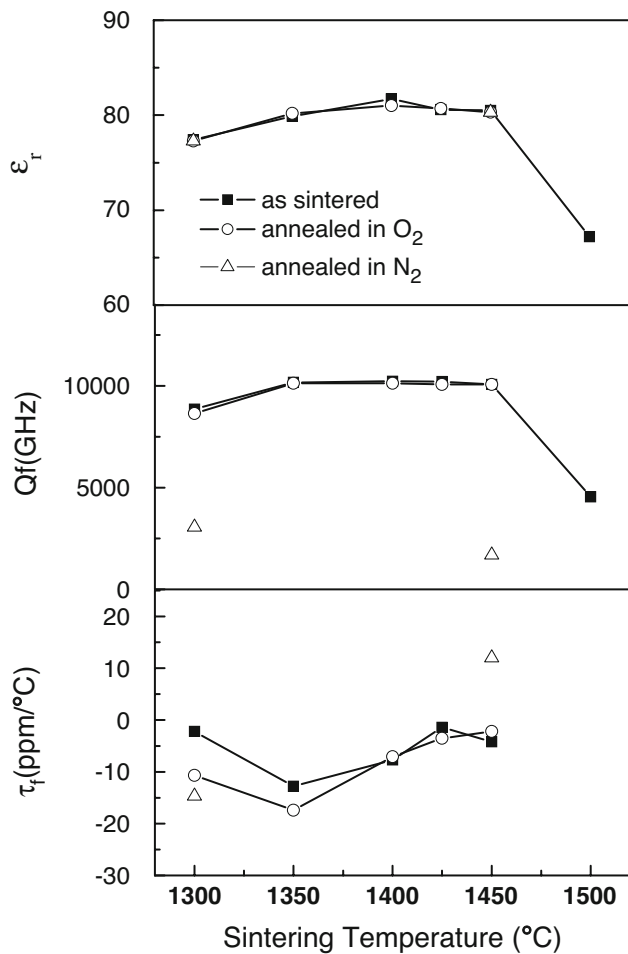


Fig. 5 Microwave dielectric properties (a) ϵ_r , (b) Qf , and (c) τ_f of $Ba_{6-3x}Sm_{8+2x}Ti_{18}O_{54}$ ($x=2/3$) ceramics

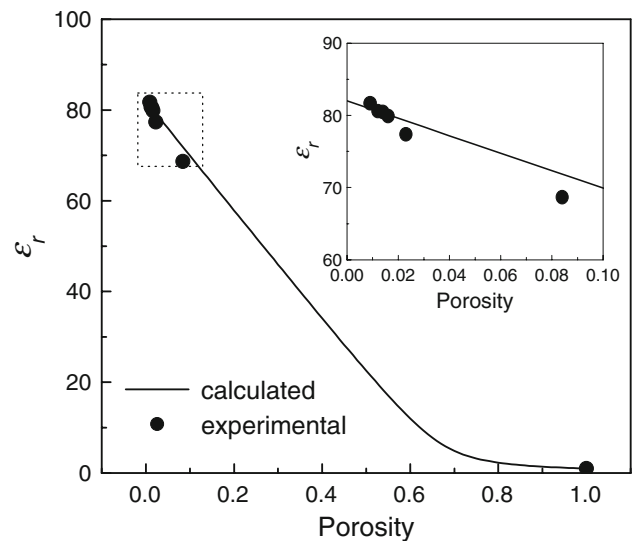


Fig. 6 Dependence of dielectric constant of $Ba_{6-3x}Sm_{8+2x}Ti_{18}O_{54}$ ($x=2/3$) ceramics on porosity at room temperature

According to the classical dispersion theory [13], the intrinsic dielectric loss of a perfect crystal originated from the anharmonic interaction of the alternating electromagnetic field with the phonon system of the crystal. In quasi-harmonic approximation, the lattice anharmonicity is described by a damp parameter γ , which is determined only by composition, crystal structure, and the temperature. In real single crystals and polycrystalline ceramics, however, the extrinsic factors such as defects, dopants, pores, and grain boundaries also contribute to the anharmonicity. Because the unique composition $Ba_{6-3x}Sm_{8+2x}Ti_{18}O_{54}$ ($x=2/3$) has been investigated in the present work, the intrinsic damping is the same for all the ceramics obtained from various sintering and annealing processes. The variation of Qf value should be related to the extrinsic factors.

Defects are strong phonon scatters. The oxygen vacancies introduced by N₂-annealing are effective on reducing the Qf value of $Ba_{6-3x}Sm_{8+2x}Ti_{18}O_{54}$ ceramics. The grain boundary, where defects, impurities, and large inner stress are usually concentrated, is another important factor to influence the Qf value. When the ceramic was sintered at 1,300°C, high density was achieved, but the grains were still small and the grain boundaries were irregular due to the insufficient grain growth. By improving the sintering temperature, the grains grew up and the total area of grain boundaries decreased. Consequently, the Qf value tends to increase with the increasing sintering temperature. On the other hand, the elongated grain grown was enhanced at higher sintering temperature, and more grain boundaries were formed in comparison with the spheric grains. As the result of the competition between the above two processes, the total area of brain boundaries is stabilized. It explains the platform on the Qf curve at 1,350~1,450°C.

The temperature coefficient of resonant frequency of $\text{Ba}_{6-3x}\text{Ln}_{8+2x}\text{Ti}_{18}\text{O}_{54}$ solid solutions is commonly determined by the phase constitution and the tilting of TiO_6 octahedra. In the present work, τ_f also exhibits some dependence on the orientation of the rod-like grains. According to the anisotropic dielectric properties reported by Wada *et al.* [8] and Hoffman *et al.* [9], the τ_f along *c*-axis is negative, whereas the value perpendicular to *c*-axis is positive. The rod-like grains elongate along the *c*-axis tend to be perpendicular to the pressing axis. With increasing sintering temperature, the orientation degree is improved. The τ_f of TE_{011} modes shifts from negative to positive.

4 Conclusions

A detailed study on the microstructures of $\text{Ba}_{6-3x}\text{Sm}_{8+2x}\text{Ti}_{18}\text{O}_{54}$ ceramics and their effects on the microwave dielectric response was performed. Dense $\text{Ba}_{6-3x}\text{Sm}_{8+2x}\text{Ti}_{18}\text{O}_{54}$ ceramics with varied grain size and grain morphologies were obtained in a wide sintering temperature range of 1,300–1,450°C. The dielectric constant changed slightly with sintering temperature in the same tendency of density. The variation of the Qf value is dominated by grain size and grain morphology. The increased grain size and larger circularity have led to the improved Qf value. τ_f exhibited a strong reliance on the orientation of the elongated grains. The inherent cation

vacancies inhibit the formation of oxygen vacancies, which have little effect on ε but have significant influence on Qf values.

Acknowledgment This work was financially supported by the Primary Project of National Science Foundation of China under grant number 50332030 and Chinese National Key Project for Fundamental Researches under grant number 2002CB613302.

References

1. H. Ohsato, J. Eur. Ceram. Soc. **21**, 2703 (2001)
2. H. Ohsato, M. Imaeda, Mater. Chem. Phys. **79**, 208 (2003)
3. X.M. Chen, Y. Li, J. Am. Ceram. Soc. **85**, 579 (2002)
4. M. Valant, D. Suvorov, C.J. Rawn, Jpn. J. Appl. Phys. **38**, 2820 (1999)
5. E.L. Colla, I.M. Reaney, N. Setter, J. Appl. Phys. **74**, 3414 (1993)
6. Y. Li, X.M. Chen, J. Eur. Ceram. Soc. **22**, 715 (2002)
7. T. Negas, P.K. Davies, Ceram. Trans. **53**, 179 (1995)
8. K. Wada, K. Kakimoto, H. Ohsato, J. Eur. Ceram. Soc. **23**, 2535 (2003)
9. C. Hoffmann, R. Waser, Ferroelectrics **201**, 127 (1997)
10. B.W. Hakki, P.D. Coleman, IRE Trans. Microwave Theor. Tech. **8**, 402 (1960)
11. A.L. Horovistiz, J.R. Frade, L.R.O. Hein, J. Eur. Ceram. Soc. **24**, 619 (2004)
12. J.P. Calame, A. Birman, Y. Carnel, D. Gershon, B. Levush, J. Appl. Phys. **80**, 3992 (1996)
13. B.D. Silverman, Phys. Rev. **125**, 1921 (1962)